Available online at www.sciencedirect.com
ScienceDirect
Nuclear Physics B Proceedings Supplement 00 (2014) 1–6
Nuclear Physics B Proceedings Supplement

Recent results on $e^+e^- \to hadrons$ cross sections from SND and CMD-3 detectors at VEPP-2000 collider.

T.V.Dimova[a,b], M.N. Achasov[a,b], R.R. Akmetshin[a,b], A.V. Anisenkov[a,b], V.M. Aulchenko[a,b], V.Sh. Banzarov[a], A.Yu. Barnyakov[a,b], N.S. Bashtovoy[a], K.I. Beloborodov[a,b], A.V. Berdyugin[a,b], D.E. Berkaev[a,b], A.G. Bogdanchikov[a], A.E. Bondar[a,b], A.A. Botov[a], A.V. Bragin[a], V.P. Druzhinin[a,b], S.I. Eidelman[a,b], D.A. Epifanov[a,c], L.B. Epshteyn[a,d], A.L. Erofeev[a], G.V. Fedotovich[a,b], S.E. Gayazov[a,b], V.B. Golubev[a,b], A.A. Grebenuk[a,b], D.N. Grigoriev[a,b,d], E.M. Gromov[a], F.V. Ignatov[a,b], L.V. Kardapoltsev[a,b], S.V. Karpov[a], A.S. Kasaev[a], V.F. Kazanin[a,b], A.G. Kharlamov[a,b], B.I. Khazin[a,b], A.N. Kirpotin[a], A.A. Korol[a,b], S.V. Koshuba[a,b], O.A. Kovalenko[a,b], D.P. Kovrizhin[a,b], A.N. Kozyrev[a], E.A. Kozyrev[a,b], P.P. Krokovny[a,b], A.S. Kupich[a,b], A.E. Kuzmenko[a,d], A.S. Kuzmin[a,b], I.B. Logashenko[a,b], P.A. Lukin[a,b], K.A. Martin[a,b], K.Yu. Mikhailov[a,b], A.E. Obrazovsky[a], V.S. Okhapkin[a], A.V. Otboev[a], E.V. Pakhtusova[a], Yu.N. Pestov[a], A.S. Popov[a,b], G.P. Razuvaev[a,b], A.A. Ruban[a], N.M. Ryskulov[a], A.E. Ryzhenenkov[a,b], A.I. Senchenko[a], S.I. Serednyakov[a,b], P.Ju. Shatunov[a], Ju.M. Shatunov[a,b], V.E. Shebalin[a,b], D.N. Shemyakin[a,b], D.A. Shtol[a], D.B. Shwartz[a,b], B.A. Shwartz[a,b], A.L. Sibidanov[a,e], Z.K. Silagadze[a,b], A.N. Skrinsky[a], E.P. Solodov[a,b], I.K. Surin[a], A.A. Talyshev[a,b], Ju.A. Tikhonov[a,b], V.M. Titov[a], Yu.V. Usov[a,b], A.V. Vasiljev[a,b], A.I. Vorobiov[a,b], Yu.V. Yudin[a,b], I.M. Zemlyansky[a]

[a] *Budker Institute of Nuclear Physics, SB RAS, Novosibirsk 630090, Russia*
[b] *Novosibirsk State University, Novosibirsk 630090, Russia*
[c] *University of Tokyo, Department of Physics, 7-3-1 Hongo Bunkyo-ku Tokyo, 113-0033, Japan*
[d] *Novosibirsk State Technical University, Novosibirsk, 630092, Russia*
[e] *University of Sidney, School of Physics, Falkner High Energy Physics, NSW 2006, Sydney, Australia*

Abstract

Recent results on various cross sections of $e^+e^- \to hadrons$ obtained with the SND and CMD3 detectors at the VEPP-2000 collider in the energy range up to 2 GeV are presented. The final states studied include $e^+e^- \to \pi^+\pi^-$, K^+K^-, $\pi^+\pi^-\pi^0$, $\pi^+\pi^-\pi^0\pi^0$, $\eta\pi^+\pi^-$, $\omega\eta$, $\eta\gamma$ and others. The measured cross sections are important since they contribute to the total hadronic cross section, muon g-2 and parameters of excited vector mesons. The nucleon-antinucleon production at threshold was also studied.

Keywords:

1. Introduction

In 2010-2013 experiments with the SND[1] and CMD-3[2] detectors were carried out at the VEPP-2000 collider [3] in the center-of-mass (c.m.) energy range from 320 MeV to 2 GeV. Each detector collected about 65 pb^{-1} of integrated luminosity including 40 pb^{-1} above the ϕ-meson mass, 8 and 7.5 pb^{-1} at the ω and ϕ resonances, respectively, and 9.5 pb^{-1} in the non-resonant region below the ϕ.

SND (Fig.1) is the general-purpose nonmagnetic detector, which consists of a nine-layer drift chamber, aerogel Cherenkov counters, three-layer spherical electromagnetic calorimeter with 1680 NaI(Tl) crystals and a muon system.

CMD-3 (Fig.2) is the general-purpose cryogenic magnetic detector. It consists of a tracking system, barrel and endcap electromagnetic calorimeters based on CsI and BGO crystals, respectively, state-of-the-art liquid Xe calorimeter and a muon-range system. The

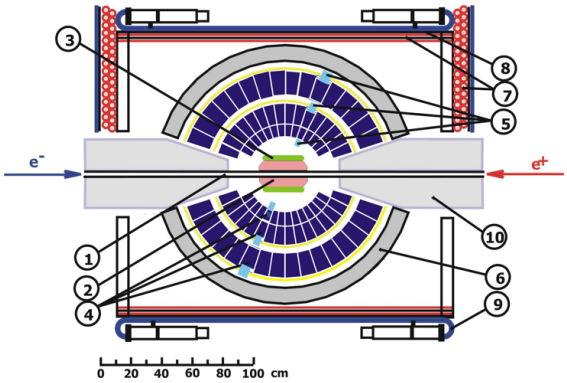

Figure 1: The SND detector: 1 - beam pipe, 2 - tracking system, 3 - aerogel Cherenkov counters, 4 - NaI(Tl) crystals, 5 - phototriodes, 6 - iron muon absorber, 7-9 - muon detector, 10 - focusing superconducting solenoids.

tracking system consists of a drift chamber and two layers of a proportional Z-chamber inside a thin superconductive solenoid with 1.5 T magnetic field.

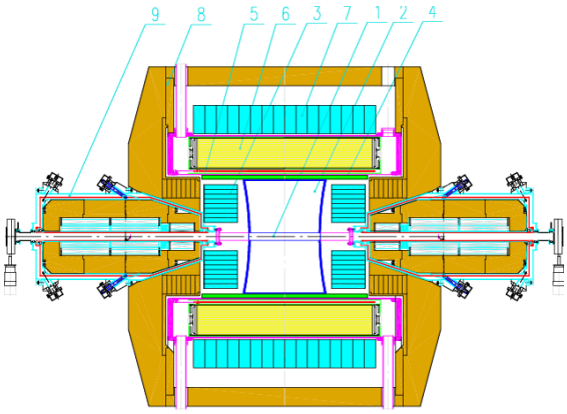

Figure 2: CMD-3 detector layout: 1 - vacuum chamber, 2 - drift chamber (DC), 3 - BGO endcap calorimeter (BGO), 4 - Z-chamber (ZC), 5 - superconducting solenoid, 6 - liquid Xe calorimeter(LXe), 7 - CsI barrel calorimeter (CsI), 8 - iron yoke, 9 - liquid He supply, 10 - vacuum pumpdown, 11 - VEPP-2000 superconducting magnetic lenses.

2. Multihadron processes

Process $e^+e^- \to \eta\gamma$.

This process was studied in the 7γ final state. This is the first measurement of the cross section in the c.m. energy range above 1.4 GeV. The obtained cross section is shown in Fig.3. The approximation was performed taking into account the $\rho(770)$, $\omega(782)$,$\phi(1020)$, $\rho(1450)$ and $\phi(1680)$ contributions.

Process $e^+e^- \to \pi^+\pi^-$.

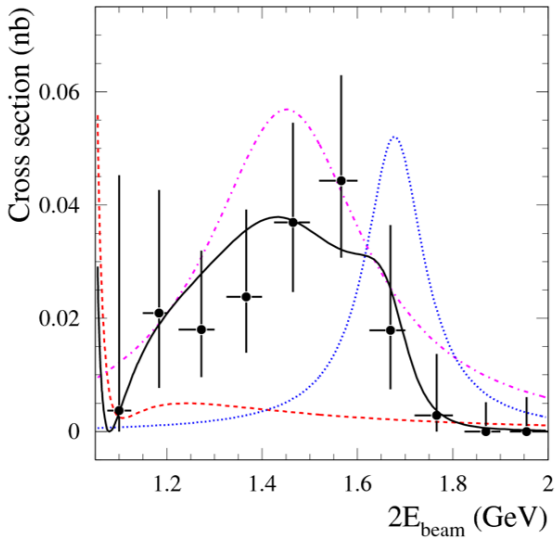

Figure 3: Cross section of the process $e^+e^- \to \eta\gamma$ obtained at SND. The solid line is the result of the approximation by a sum of the $\rho(770)$, $\omega(782)$,$\phi(1020)$, $\rho(1450)$ and $\phi(1680)$ contributions. The dashed line - calculated cross section with the $\rho(770)$, $\omega(782)$,$\phi(1020)$ contributions only, dash-dotted line - the $\rho(1450)$ contribution, dotted line - that of the $\phi(1680)$.

The dominant contribution to R(s) in the c.m. energy range $\sqrt(s) < 1$ GeV comes from the $e^+e^- \to \pi^+\pi^-$ mode. A preliminary result on the form factor obtained at CMD-3 is shown in Fig.4. The geometry of this process allows to perform clean selection of $e^+e^- \to e^+e^-$, $e^+e^- \to \mu^+\mu^-$, $e^+e^- \to \pi^+\pi^-$ collinear events practically without physical background. These final states can be separated using either information about energy deposition in the calorimeter or that about particle momenta in the drift chamber at $E_{beam} \leq$360 MeV. The two methods overlap in the energy range 160÷ 360 MeV allowing their cross-check. The layered structure of the LXe calorimeter allows to perform MVA analysis of the longitudinal shower profile, which should help to keep a systematic error of event separation at the level of 0.2%. The goal of the CMD-3 experiment is to reduce the total systematic uncertainty in this channel to 0.35%.

Process $e^+e^- \to K^+K^-$.

This process was studied with SND in the energy range from 1.05 to 2.0 GeV. Kaons were selected using information from aerogel Cherenkov counters. The obtained cross section in comparison with BABAR data[5] is shown in Fig.5. Both cross sections are in good agreement and have the same level of statistical accuracy. The complicated shape of the cross section is related to the interference of all excited vector resonances in this re-

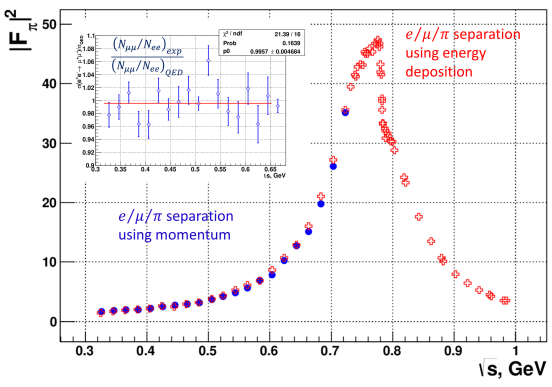

Figure 4: Form factor of the $e^+e^- \to \pi^+\pi^-$ process obtained at CMD-3. Open crosses, red - $e/\mu/\pi$ separation using the calorimeter data, filled curcles, blue – using the tracker data. The inset shows the ratio of the measured $e^+e^- \to \mu^+\mu^-$ cross section to the QED expectation for the analysis based on the tracker data.

gion, which includes both isovector and isoscalar states.

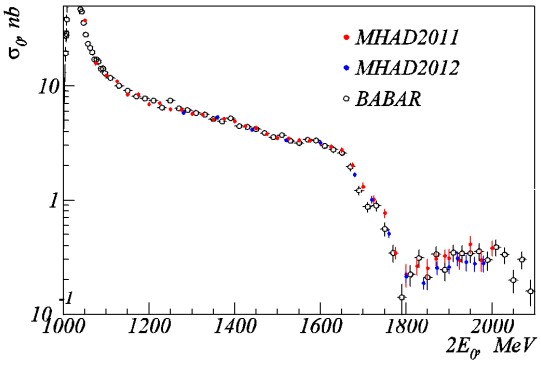

Figure 5: Cross section of the process $e^+e^- \to K^+K^-$ obtained at SND in comparison with BABAR data

Process $e^+e^- \to K^+K^-\pi^+\pi^-$.

The preliminary CMD-3 results on the $e^+e^- \to K^+K^-\pi^+\pi^-$ cross section in comparison with BABAR [6] are shown in Fig.6. This channel has rich dynamics with many intermediate states like: $K^*(1270)K \to K^*(892)K\pi$, $K^*(1400)K \to K^*(892)K\pi$, $K^*(1270)K \to \rho KK$, $K^*(892)K^*(892)$, $\phi\pi\pi$. Figure7 shows dominance of the $K^*(892)$ intermediate state in the $K\pi$ invariant mass and presence of the ρ and ϕ resonances in the $\pi^+\pi^-$ and K^+K^- combinations, respectively.

Process $e^+e^- \to \pi^+\pi^-\pi^+\pi^-$.

This process has one of the largest cross sections in the energy region from 1 to 2 GeV. The cross section measured by CMD3 is shown in Fig.8 and is in good

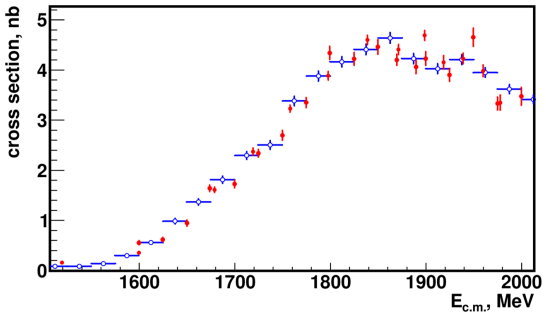

Figure 6: Cross section of the process $e^+e^- \to K^+K^-\pi^+\pi^-$ obtained by CMD-3 in comparison with BABAR data

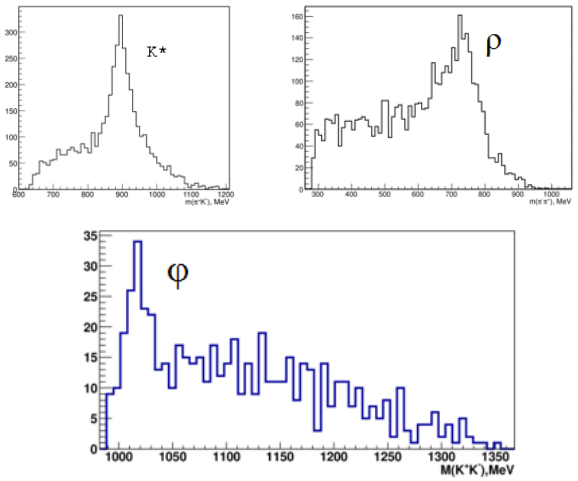

Figure 7: Invariant mass spectra for the $K\pi$, $\pi\pi$ and KK systems

agreement with BABAR[7]. The statistical error is at the level of 1-2% per point.

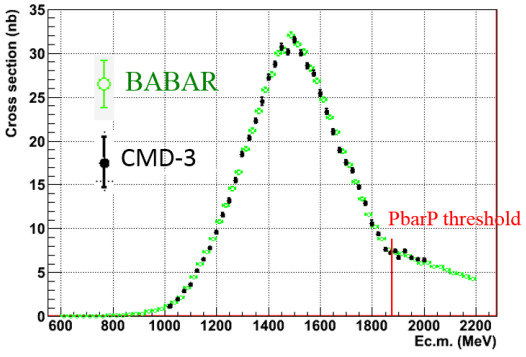

Figure 8: Cross section of the process $e^+e^- \to \pi^+\pi^-\pi^+\pi^-$ obtained at CMD-3 in comparison with BABAR data

Process $e^+e^- \to 3(\pi^+\pi^-)$.

The cross section measured by CMD3 (Fig.9 is in good agreement with BABAR[8]. The ratio of the five and six track events was used to estimate the model-dependent uncertainty in the acceptance calculation. From this study it was concluded that the observed production mechanism can be described by the production of one $\rho(770)$ resonance with four remaining pions in the S-wave distributed according to phase space. It was also observed that the production dynamics changes in the 1850-1900 MeV c.m. energy range and demands a further study.

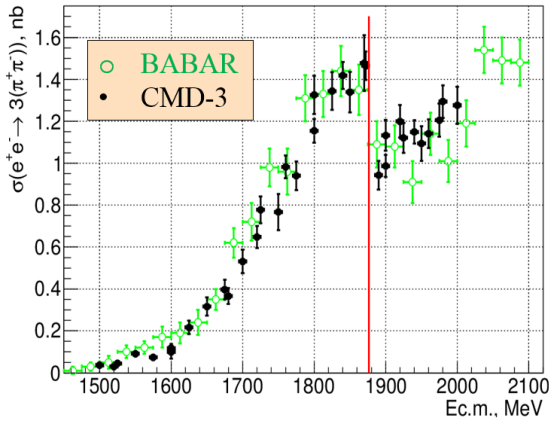

Figure 9: Cross section of the process $e^+e^- \to 3(\pi^+\pi^-)$ obtained at CMD-3 in comparison with BABAR data

Process $e^+e^- \to 2(\pi^+\pi^-\pi^0)$.

The preliminary result on the cross section of $e^+e^- \to 2(\pi^+\pi^-\pi^0)$ measured at CMD-3 is shown in Fig.10. It is in reasonable agreement with BABAR data[8]. A dip in both $e^+e^- \to 3(\pi^+\pi^-)$ and $e^+e^- \to 2(\pi^+\pi^-\pi^0)$ cross sections is seen near the $p\bar{p}$ threshold.

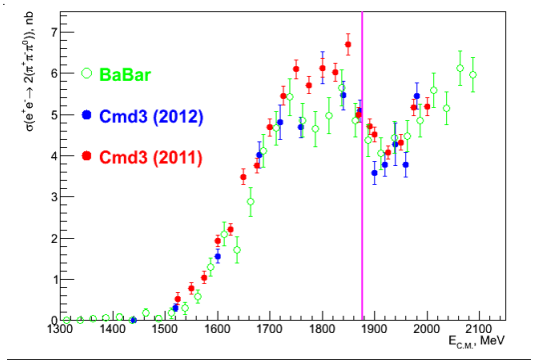

Figure 10: Cross section of the process $e^+e^- \to 2(\pi^+\pi^-\pi^0)$ obtained at CMD-3 in comparison with BABAR data

Process $e^+e^- \to \pi^+\pi^-\pi^0$.

The measured $e^+e^- \to \pi^+\pi^-\pi^0$ cross section in comparison with the previous SND[9] and BABAR[10] data is shown in Fig.11. This is the most accurate result. The approximation was performed taking into account the contributions from the $\omega(782)$, $\phi(1020)$, $\omega'(1420)$ and $\omega''(1650)$ resonances. To describe the cross section above 1.8 GeV, the non-resonant contribution or additional excited resonance should be taken into account.

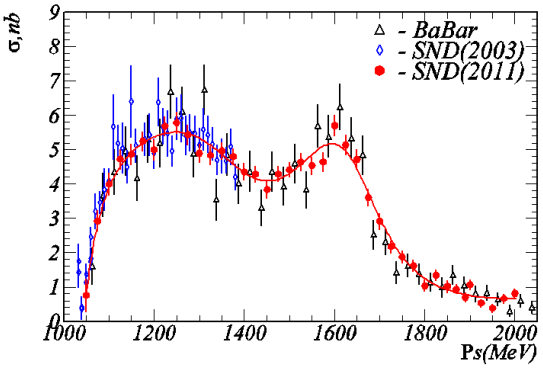

Figure 11: Cross section of the process $e^+e^- \to \pi^+\pi^-\pi^0$ obtained at SND in comparison with the previous SND and BABAR data

Process $e^+e^- \to \pi^+\pi^-\eta$.

This process was studied at SND in the $\eta \to 2\gamma$ decay mode. The measured cross section in comparison with previous results is shown in Fig.12. The fit of the cross section was done by a sum of the $\rho(770)$, $\rho(1450)$ and $\rho(1700)$ contributions. Using SND data and CVC hypothesis the probability of $\tau \to \eta\pi^-\pi^0\nu_\tau$ decay was calculated to be $B(\tau \to \eta\pi^-\pi^0\nu_\tau) = (0.180 \pm 0.048)\%$. This value is in reasonable agreement with the PDG[4] data: $B(\tau \to \eta\pi^-\pi^0\nu_\tau) = (0.139 \pm 0.010)\%$.

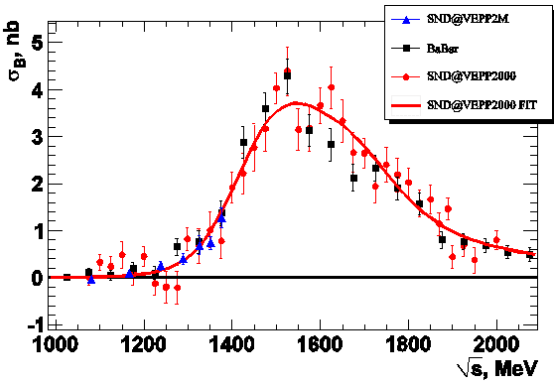

Figure 12: Cross section of the process $e^+e^- \to \pi^+\pi^-\eta$ obtained at SND in comparison with the previous SND[11] and BABAR data[12]

Process $e^+e^- \to \pi^+\pi^-\pi^0\eta$.

The preliminary result on the cross section of the process $e^+e^- \to \pi^+\pi^-\pi^0\eta$ at SND is shown in Fig.13. This is the first measurement of the cross section of this process in the wide energy range. The cross section can be described by a sum of contributions from the $\omega(1650)$ and $\phi(1680)$ resonances. This process has several intermediate states. Two of them ($\omega\eta$ and $\phi\eta$) can be seen at the η-meson recoil spectrum (Fig.14). They were also studied at BABAR detector[8, 13] using other final states. Contributions of some other intermediate states are under study.

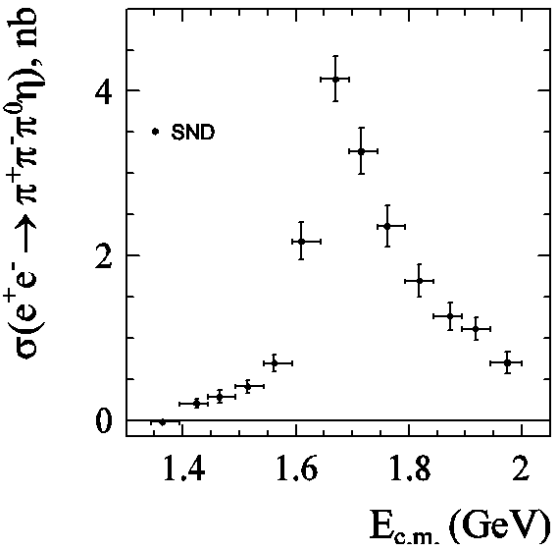

Figure 13: Cross section of the $e^+e^- \to \pi^+\pi^-\pi^0\eta$ process obtained at SND

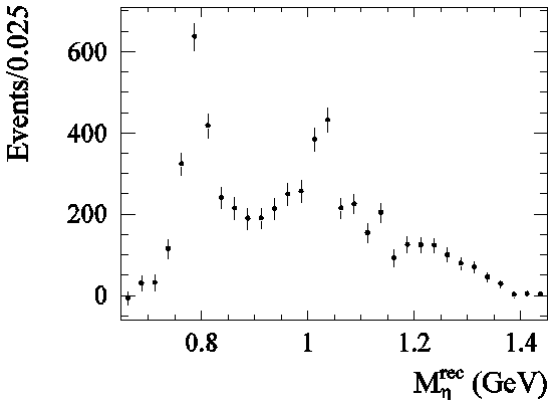

Figure 14: Recoil mass spectrum of η meson

Process $e^+e^- \to p\bar{p}$.

The cross section of $e^+e^- \to p\bar{p}$ was measured at the SND and CMD-3 detectors in the near-threshold region (Fig.15,16). The analysis was done on the base of a 10 pb^{-1} data set. There is no contradiction with previous data.

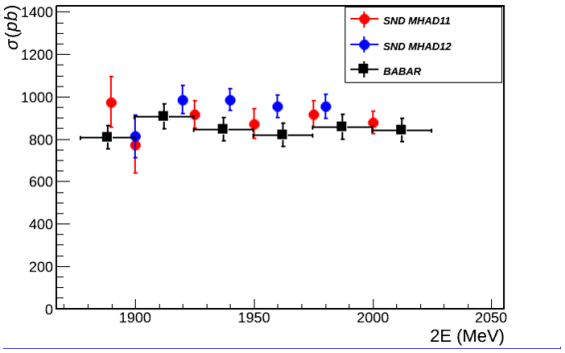

Figure 15: Cross section of the process $e^+e^- \to p\bar{p}$ obtained at SND in comparison with BABAR[14]

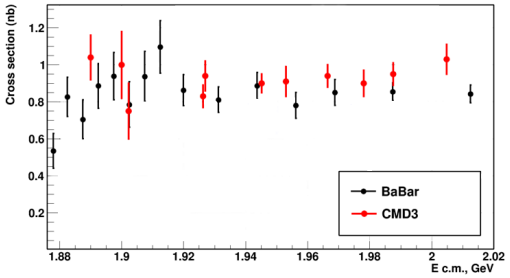

Figure 16: Cross section of the process $e^+e^- \to p\bar{p}$ obtained at CMD-3 in comparison with BABAR[14]

Process $e^+e^- \to n\bar{n}$.

The cross section of $e^+e^- \to n\bar{n}$ was measured in the near-threshold region (Fig.17). The result is in good agreement with previous data obtained in the FENICE experiment[15].

The cross sections of the processes $e^+e^- \to p\bar{p}$ and $e^+e^- \to n\bar{n}$ can be descibed in terms of the effective form factor. Energy dependence of the effective form factor for neutrons obtained from the SND $e^+e^- \to n\bar{n}$ cross section in comparison with FENICE data for neutrons and BABAR result for protons is shown at Fig.18

3. Conclusions

Since 2010 the VEPP-2000 e^+e^--collider accumulated about 65 pb^{-1} of data with each of the SND and

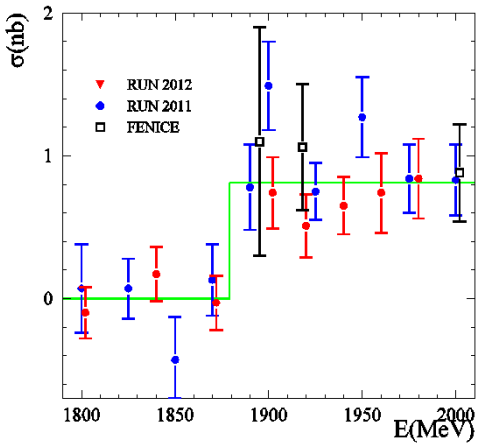

Figure 17: Cross section of the process $e^+e^- \to n\bar{n}$ obtained at SND

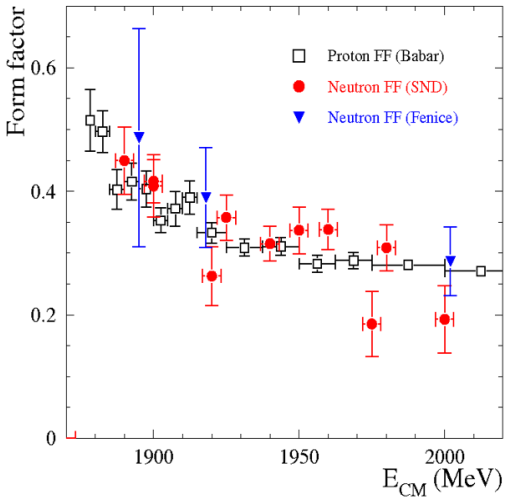

Figure 18: Comparison of nucleon and proton form factors obtained from SND, BABAR and Fenice data

CMD-3 detectors in the range E=0.3÷2 GeV. Data analysis of meson and nucleon production is in progress. The obtained results have the same or better statistical precision than previous experiments. After VEPP-2000 upgrade, data taking will resume in 2015 with the goal of collecting 1 fb^{-1} of integrated luminosity.

4. Acknowledgments

This work is partially supported in the framework of the State order of the Russian Ministry of Science and Education, Federal Program ‘Scientific and teaching personnel of innovative Russia” (2009 – 2013), Agreement 14.B37.21.07777 and by RFBR grants No. 12-02-00065-a, 12-02-01250-a, 12-02-01032-a, 12-02-31498-a, 12-02-31499-a, 12-02-31501-a, 13-02-00375, 13-02-00418-a, 13-02-00215-a, 13-02-01134-a, 14-02-00129-, 14-02-00047-a, 14-02-00580-a, 14-02-31375-mol-a, 14-02-31478-mol and scientific school grant 2479.2014.2.

References

[1] M.N. Achasov *et al.*, *Nucl. Instrum. Meth.***A598**, 31 (2009).
V.M. Aulchenko et al., *Nucl. Instrum. Meth.***A598**, 102 (2009).
[2] V. M. Aulchenko et al., BUDKER-INP-2001-45
B. Khazin,Nucl. Phys. Proc. Suppl. 181-182 (2008) 376.
[3] Yu.M. Shatunov *et al.*, Project of a new electron positron collider VEPP-2000 in *Proc. of the 7th European Particle Accelerator Conference* (Vienna, Austria, 2000), p. 439.
[4] J.Beringer *et al.* (Particle Data Group), *Phys. Rev. D* **86**, 010001 (2012).
[5] J. P. Lees *et al.* (BABAR Collaboration), *Phys. Rev. D* **88**, 032013 (2013).
[6] B. Aubert *et al.* (BABAR Collaboration) *Phys. Rev. D* **76**, 012008 (2007).
[7] B. Aubert *et al.* (BABAR Collaboration) *Phys. Rev. D* **71**, 052001 (2005)
[8] Aubert *et al.* (BABAR Collaboration) *Phys. Rev. D* **73**, 052003 (2006).
[9] M. N. Achasov *et al. Phys. Rev. D* **66** , 032001 (2002)
[10] Aubert *et al.* (BABAR Collaboration) *Phys. Rev. D* **70**, 072004 (2004).
[11] M.N.Achasov *et al.*, *JETP Lett.* **92**, 84 (2010).
[12] B.Aubert *et al.* (BABAR Collaboration) *Phys. Rev. D* **76**, 092005 (2007).
[13] B. Aubert *et al.* (BABAR Collaboration) *Phys. Rev. D* **77**, 092002, (2008).
[14] B. Aubert *et al.* (BABAR Collaboration) *Phys. Rev. D* **73**, 012005 (2006).
[15] A.Antonelli *et al.*, *Phys. Lett. B* **313**, 283 (1993).